

COMPARISON OF IDEAL STAGE AND MASS TRANSFER MODELS FOR SEPARATION PROCESSES WITH AND WITHOUT CHEMICAL REACTIONS

Christopher Skowlund, Ph.D.
Michael Hlavinka, Ph.D., P.E.
Mauricio Lopez, Ph.D.
Bryan Research & Engineering, Inc.
Bryan, TX, U.S.A.

Carl Fitz, Ph.D., P.E.
S-Con Inc.
Bryan, TX, U.S.A.

ABSTRACT

The design and optimization of separation processes is carried out using process simulators which utilize various calculation approaches. Two techniques which are widely used for modeling distillation are the ideal stage model and the mass transfer model. The ideal stage model is relatively simple, but requires an overall efficiency for trays or a height equivalent of a theoretical stage for packing. The mass transfer model is significantly more computationally intensive and relies heavily on empirical equations for properties such as diffusivity, mass transfer coefficients and interfacial area.

The primary emphasis of this paper will be on the application and comparison of the ideal stage and mass transfer models to systems with and without chemical reactions such as amine treating, glycol dehydration, reactive distillation and hydrocarbon separation columns. The advantages and disadvantages of each method will be discussed along with recommended guidelines for their application and use.

COMPARISON OF IDEAL STAGE AND MASS TRANSFER MODELS FOR SEPARATION PROCESSES WITH AND WITHOUT CHEMICAL REACTIONS

INTRODUCTION

Distillation plays an important role in many industrial chemical plants, but for most engineers the understanding of the complex phenomena occurring in a distillation column tends to be limited to the simplest of models. One reason for this is that most undergraduate and graduate programs tend to gloss over these complexities due to the time it would require to thoroughly cover the topic. Another reason is that the simple models often tend to provide reasonably accurate results for relatively little work.

Over the past 30 years advances in the computing power available to most engineers has allowed more complex distillation models to be implemented in commercial process simulation software. A similar increase in the utilization of distillation columns to reliably perform separations which also incorporate ionic and molecular reactions has required the engineer to demand more of their simulation software. Although most engineers are not required to understand the intricacies of the mathematical models used to solve the most complex columns, it is important to understand the differences between the simpler ideal stage models and the more detailed mass transfer models or nonequilibrium stage models. Due to limitations inherent in the assumptions used to derive each model and the data required to accurately perform the calculations, neither model can be assumed to work best in all situations. But, with suitable experience and guidance, engineers can now be expected to provide reliable designs for a wider range of columns than in the past.

Obviously, the main disadvantage of the ideal stage approach is just that—the use of ideal stages to model real trays or packing depths. However, for most processes encountered in gas processing and other industries, the overall efficiencies are well established for properly operating conditions of the column. For systems that are unavailable, similar systems often exist to allow for efficiency estimation. If not, the mass transfer approach is available as an option.

The primary feature with the mass transfer approach to the end user is the ability to model a column with the actual number of trays in the unit or the actual depth of packing. However, as will be discussed later, there are still several assumptions that are made in this approach that can have a significant impact on results. Two that are worth mentioning at this point include the mixing model for trayed columns and the discretization of the packing depth for packed towers. If the simulator allows the user to select from various alternatives for these parameters, knowing *a priori* the correct selection is problematic. If the values are fixed within the simulator, how does the user know for sure that proper values are selected for a given system? Further, the prediction of multicomponent mass transfer coefficients is of questionable accuracy. These facts lead us to recommend that columns modeled with the mass transfer approach be checked against an ideal stage model with an expected efficiency until you have sufficient experience with the particular application.

All simulation results presented in this paper were made using the upcoming major release of BR&E ProMax[®] [1] which will be known as ProMax 4.0. ProMax offers the ability to use either the ideal stage or the mass transfer approach at the discretion of the user. These approaches can be applied to a wide variety of processes, with and without reactions, as will be seen in the examples that are presented later.

MODEL BACKGROUND

In this section, the basic concepts behind the ideal stage model and the mass transfer model are presented. In addition, some of the principal assumptions in each approach are given.

Ideal Stage Models

Chemical engineers have been modeling distillation columns using the ideal stage model for over a century [2]. The ideal stage model is easy to use as a detailed equipment design is not required. The ideal stage model requires a minimum amount of data—only equilibrium relationships and enthalpy data for the heat balance. These are solved along with a material balance for each component and the requirement that the mole fractions in each phase sum to one. These are often referred to as the MESH (Mass, Equilibrium, Summation and Heat) equations. A graphical technique which solves the material and energy balance assuming equilibrium is the Ponchon-Savarit [3, 4] diagram. If constant molar overflow is assumed, enthalpy data are not required. The popular McCabe-Thiele [5] graphical method is an example of this approach. The ideal stage model is the fastest way to make stage-to-stage calculations. However, convergence becomes more difficult as the equilibrium and enthalpy data become more dependent on composition, temperature, or pressure.

The assumptions of the ideal stage approach are that the vapor and liquid are both perfectly mixed so that the vapor and liquid leaving a stage are at the same composition as the material on the stage, and that thermodynamic equilibrium is obtained on each stage. Columns often do not operate under these conditions. The equilibrium assumption also means liquid and vapor leaving a stage are at the same temperature—a reasonable approximation for many industrial columns. The equilibrium assumption also means that the mole fractions of each component leaving a stage are related by the well-known expression:

$$K_i = \frac{y_i}{x_i} = \frac{\hat{\phi}_i^L}{\hat{\phi}_i^V} \quad (1)$$

where K_i represents the thermodynamic equilibrium constant for component i , and y_i and x_i are the mole fractions of the vapor and liquid, respectively, for component i . The $\hat{\phi}_i^L$ and $\hat{\phi}_i^V$ terms represent the fugacity coefficient for component i in the liquid and vapor phases, respectively. The thermodynamic equilibrium constant is normally obtained from a variety of methods depending on the system complexity. For most gas processing applications this will be from an equation of state, which yields the fugacity coefficients directly. However, some applications will require a Gibbs excess free energy model which provides the fugacity coefficients through activity coefficients when the liquid phase becomes more non-ideal.

In general, the constant K_i represents the relationship between the vapor and liquid phase compositions at any point in the column. One method of accounting for non-ideal column performance is to adjust the value of K_i away from the thermodynamic equilibrium value of equation (1) by incorporating the phenomena occurring in the column (*e.g.*, imperfect mixing on a tray or back-mixing in a packed column) into a model for K_i while continuing to use the ideal stage model to satisfy the MESH equations. This is the approach taken by application of tray efficiency as shown below. Other methods utilize the ideal model with the equilibrium K_i and then adjust the required number of trays or packing height to account for column non-idealities.

Ideal stage models can also account for non-ideal column performance through the use of reaction kinetics, as is done in the TSWEET kinetics option of ProMax [1]. TSWEET modifies carbon

dioxide absorption by taking into account the effect ionic dissociation kinetics have on the amount of carbon dioxide which can be absorbed by a column based on the column design, inlet conditions, etc.

Overall Efficiency

In order to use the ideal stage approach with columns that do not operate under the ideal assumptions stated above, one of several types of efficiency approaches is normally used. The most commonly used column efficiency is the overall column efficiency E_o which relates the number of actual trays N_A to the number of theoretical (or equilibrium) trays N_T as:

$$N_A = \frac{N_T}{E_o} \quad (2)$$

Several techniques can be used to apply overall efficiencies to distillation columns. The simplest technique is to assume the overall efficiency is constant throughout the entire column. For many gas processing applications, this approach is satisfactory. Table I, taken from the GPSA Engineering Data Book [6, 7], provides values that are commonly used in the gas processing industry. Overall efficiencies for other systems are usually estimated from similar chemical systems where the overall efficiency is known, from application experience of the design team, from experimental results obtained in laboratory distillations, or from correlations such as that of O'Connell [8].

Table I - Typical Tray and Packing Efficiencies [6,7]

| Application | Typical Tray Efficiency (%) | Packing Type | HETP (ft) | Reference |
|-----------------------|------------------------------------|---------------------|------------------|------------------|
| Demethanizer | 45-60 | | | 6 |
| Deethanizer top | 60-75 | 1.5 inch Pall Rings | 2.9 | 6 |
| Deethanizer bottom | 60-75 | 2 inch Pall Rings | 3.3 | 6 |
| Depropanizer top | 80-90 | 1.5 inch Pall Rings | 3.2 | 6 |
| Depropanizer bottom | 80-90 | 1.5 inch Pall Rings | 2.4 | 6 |
| Debutanizer top | 85-95 | 1.5 inch Pall Rings | 2.4 | 6 |
| Debutanizer bottom | 85-95 | 1.5 inch Pall Rings | 2 | 6 |
| Butane Splitter | 90-100 | | | 6 |
| Condensate Stabilizer | 50-75 | | | 6 |
| Glycol Contactor | 25-30 | Structured Packing | 5 | 7 |

As the distillation system becomes more complex where a larger number of feeds, side draws, or chemical components are involved, the overall efficiency must be applied separately to various sections of the column since a single efficiency will normally not be adequate. This type of efficiency is typically known as a sectional efficiency. Different sectional efficiencies are frequently applied between different feed trays and other areas of the column where the efficiency is expected to change.

For packed columns, the Height Equivalent to a Theoretical Plate (HETP) approach is typically used to obtain the number of theoretical trays to be used in an ideal stage simulation for the corresponding height. HETP can normally be estimated for a specified column service based on the type of packing involved. Table I presents typical HETP values that can be expected in several gas processing applications. When HETP values are not readily available, they are usually estimated from similar systems or obtained from the packing vendor.

Murphree Efficiency

Unfortunately, the overall tray efficiency approach cannot be integrated into the equilibrium relationships that are needed to solve a distillation column using the ideal stage approach. For this

purpose Murphree [9] efficiencies are typically used. For each component i on tray n , the Murphree vapor tray efficiency $E_{MV,n,i}$ is given by

$$E_{MV,n,i} = \frac{\bar{y}_{n,i} - y_{n+1,i}}{y_{n,i}^* - y_{n+1,i}} \quad (3)$$

where $\bar{y}_{n,i}$ represent the average composition of the vapor above the froth for component i on tray n and $y_{n,i}^*$ the vapor composition that would be in equilibrium with the liquid composition $x_{n,i}$ leaving the tray. In equation (3), the trays are numbered from top to bottom, and the vapor entering the tray is assumed to be well mixed. A similar equation can be expressed for the Murphree liquid tray efficiency $E_{ML,n,i}$ based on liquid compositions. In general, the liquid and vapor Murphree efficiencies are not equal. The Murphree efficiency allows for easy use in graphical solutions to distillation such as McCabe-Thiele, as it was originally used for this purpose. The differences that appear in the numerator and denominator have direct representation of line segments lengths in McCabe-Thiele.

By rearranging equation (3) the Murphree efficiency directly integrates into the equilibrium equations of the stage via

$$K_{n,i} = \frac{\bar{y}_{n,i}}{x_{n,i}} = E_{MV,n,i} K_{n,i}^{eq} + (1 - E_{MV,n,i}) \frac{y_{n+1,i}}{x_{n,i}} \quad (4)$$

where $K_{n,i}^{eq}$ is the thermodynamic equilibrium constant as calculated by equation (1). This $K_{n,i}$ can then be used in the MESH equations to model the complete column.

When the assumption of perfectly mixed liquid on a tray cannot be met, models of liquid flow from the inlet downcomer to the outlet downcomer have to be derived resulting in concentration gradients in the liquid and vapor phases. Most of these assume plug flow in the liquid phase as more complicated models cannot typically be extended from binary systems to multicomponent systems. For the case of plug flow in the liquid, a differential vertical segment of flow is analyzed, and material balance equations are written for this segment. In this differential segment, the liquid is assumed to be perfectly mixed in the vertical direction. Consequently, the vapor in equilibrium with the liquid $y_{n,i}^*$ is constant. For the segment, a Murphree vapor phase point efficiency $E_{OV,n,i}$ can be calculated as

$$E_{OV,n,i} = \frac{y_{n,i} - y_{n+1,i}}{y_{n,i}^* - y_{n+1,i}} \quad (5)$$

where $y_{n,i}$ represents the point composition for component i in the vapor of the froth immediately above the differential segment.

In practice, the Murphree point efficiency is usually calculated from a binary data correlation based on the type of tray. An example of this correlation is the AIChE *Bubble Tray Design Manual* [10]. The AIChE correlation provides the number of liquid and vapor phase transfer units, N'_L and N_V . (The prime indicator on the liquid transfer units is used to denote that it is based on a different tray model than used for the vapor transfer units. See Lockett [11] for details.) Other correlations (e.g., Zuiderweg [12]) yield liquid and vapor phase mass transfer coefficients and interfacial area independently, k_L , k_V , and a . The product of the mass transfer coefficient with the interfacial area is called the volumetric mass transfer coefficient. Finally, other correlations directly give the volumetric mass transfer coefficients, $k_L a$ and $k_V a$ [13]. For the latter two types of correlations, the number of liquid and vapor transfer units is calculated through the volumetric mass transfer coefficient. From the

number of liquid and vapor transfer units, the number of overall vapor phase transfer units N_{OV} is calculated by summing the vapor and liquid phase resistances

$$\frac{1}{N_{OV}} = \frac{1}{N_V} + \frac{\lambda}{N'_L} \quad (6a)$$

$$\lambda = \frac{mV}{L} \quad (6b)$$

which is used with

$$E_{OV} = 1 - \exp(-N_{OV}) \quad (7)$$

to obtain the Murphree vapor phase point efficiency. In equation (6b), m represents the slope of the equilibrium line, and V and L the molar vapor and liquid flow rates through the tray, respectively. When extended to multicomponent mixtures, equations (6) and (7) become matrix operations of dimension $(c-1) \times (c-1)$ since there are $c-1$ independent molar fluxes and, consequently, efficiencies. More information on the mass transfer correlations will be given later in this paper.

From the Murphree point efficiency, an appropriate liquid flow model for the tray is applied to obtain the Murphree tray efficiency E_{MV} . One such model is that of perfect mixing in which the point and tray efficiencies become equal. Lewis [14] was the first to derive an expression for the Murphree tray efficiency from the Murphree point efficiency based on liquid plug flow and a perfectly mixed vapor entering the tray. The expression obtained is:

$$E_{MV} = \frac{\exp(E_{OV}\lambda) - 1}{\lambda} \quad (8)$$

Toor [15] later derived an approach that can be used to calculate the Murphree tray efficiency for multicomponent systems using the same liquid plug flow model used by Lewis.

For a binary system, the number of overall vapor phase transfer units N_{OV} is a scalar positive value. Consequently, the Murphree vapor phase point efficiency must be bounded by $0 \leq E_{OV} \leq 1$, which is evident from equation (7). This can also be seen by inspection of equation (5) since $y_{n,i} \leq y_{n,i}^*$ in a binary system. However, equation (8) shows that the $E_{MV} \geq E_{OV}$ since $\lambda > 0$. Equation (8) also indicates that E_{MV} can be greater than 100%. This fact is due to the concentration gradients on the tray.

The above analysis is complicated greatly when extended to multicomponent systems. As stated earlier, \mathbf{N}_{OV} is a matrix of number of overall vapor phase transfer units rather than a scalar value. Multicomponent systems can have various diffusion regimes that are not possible in binary systems. These are due to the interaction effects between components where the diffusion flux of a component depends on the multicomponent diffusion coefficients and the concentration gradients of all components in the system, not just its own gradient. For example, it is possible for a component to diffuse when there is no concentration gradient for the component (osmotic diffusion), to not diffuse when a concentration gradient does exist (diffusion barrier), and to diffuse in the opposite direction of its concentration gradient (reverse diffusion). This can be seen from the multicomponent representation of Fick's Law:

$$\mathbf{J} = -\mathbf{DVC} \quad (9)$$

where \mathbf{J} is a vector of diffusion fluxes, \mathbf{D} is a square matrix of multicomponent diffusion coefficients, and $\nabla\mathbf{C}$ is a vector of concentration gradients. If \mathbf{D} is a diagonal matrix each component flux term J_i is dependent only the corresponding concentration gradient for component i . But, if \mathbf{D} is a full matrix (as it must be due to the definition of diffusivity) then each J_i is dependent on all of the concentration gradients in $\nabla\mathbf{C}$. Similarly, only when the matrix \mathbf{Q} defined by (compare to equation (7))

$$\mathbf{Q} = \exp(-\mathbf{N}_{ov}) \quad (10)$$

is a diagonal matrix with near equal values will the efficiencies be equal as in the binary system. This will only occur when the components involved are very similar, such as isomers. In general, with a full matrix, the range for Murphree point efficiencies, and consequently tray efficiencies, is $-\infty$ to $+\infty$. They can be negative or positive and are unbounded (see Taylor and Krishna [16]).

The above discussion means that you cannot attempt to justify multicomponent Murphree efficiencies in the context of binary efficiencies. The values cannot be related quantitatively to isolated binary pairs present in the multicomponent mixture since this analysis neglects the contribution of the cross terms to the efficiencies.

Unfortunately, no technique exists to relate Murphree efficiencies E_{MV} with overall column or section efficiencies E_o . Only for the simplest case of straight equilibrium lines and straight operating lines in a binary system has this been done and is given by Lewis [14] as

$$E_o = \frac{\ln[1 + E_{MV}(\lambda - 1)]}{\ln \lambda} \quad (11)$$

For more information on Murphree efficiencies and diffusional topics for binary and multicomponent systems, the reader is encouraged to refer to the texts of Lockett [11], Taylor and Krishna [16], and Bird, et al. [17].

In addition to Murphree tray efficiencies, other types of efficiencies exist. Other tray efficiencies include terms based on overall material flow rates, component flow rates, enthalpies, and temperatures. For example, the temperature based efficiencies will cause the vapor and liquid leaving a tray to exit at different temperatures. See Lockett [11] for a summary of various efficiencies.

Mass Transfer Models

In a series of papers in 1985, Krishnamurthy and Taylor [18, 19, 20] presented the initial formulation of the mass transfer or nonequilibrium stage models for distillation. These models forgo the use of efficiencies and attempt to model columns using the actual number of trays or packing heights (although packed columns are typically modeled as a specified number of discrete segments). They accomplish this by calculating the actual rates of interphase mass and heat transfer in the column. Based on the two film model, the molar rate of mass transfer for component i from the bulk vapor to the vapor-liquid interface on any stage n is

$$N_{n,i}^V = a_n k_{n,i}^V (y_{n,i}^V - y_{n,i}^I) \quad (12)$$

and the molar rate of mass transfer from the vapor-liquid interface into the bulk liquid is

$$N_{n,i}^L = a_n k_{n,i}^L (x_{n,i}^I - x_{n,i}^L) \quad (13)$$

where a_n is the interfacial area, and $k_{n,i}^V$ and $k_{n,i}^L$ are the binary vapor and liquid phase mass transfer coefficients, respectively. The superscripts I , V , and L applied to mole fraction quantities in the above equations indicate compositions at the interface, in the bulk vapor, and in the bulk liquid, respectively. At the interface, the vapor and liquid fluxes are equal so there is no accumulation of material at the interface. In reality, more complicated models of mass transfer are normally required to take into consideration the interactions between the components in a multicomponent system [21] resulting in matrices of mass transfer coefficients on each stage and separate terms for the diffusion flux and convective flux. An analogous relationship for the energy flux can also be formulated:

$$E_n^V = a_n h_n^V (T_n^V - T_n^I) + \sum_{i=1}^c N_{n,i}^V \bar{H}_{n,i}^V \quad (14)$$

$$E_n^L = a_n h_n^L (T_n^I - T_n^L) + \sum_{i=1}^c N_{n,i}^L \bar{H}_{n,i}^L \quad (15)$$

where h_n^V and h_n^L represent the vapor and liquid heat transfer coefficients, $\bar{H}_{n,i}^V$ and $\bar{H}_{n,i}^L$ are the partial molar enthalpies of component i in the vapor and liquid phases, and T_n represent the temperatures at the location denoted by the superscripts as in equations (12) and (13). The above energy formulation indicates that the temperatures of the two bulk phases will not be equal. At the interface, thermodynamic equilibrium is assumed. Therefore, the vapor and liquid temperatures at the interface are equal and the compositions are related by equation (1). Requiring the summation of the vapor and liquid mole fractions at the interface to be unity adds two additional equations to the system. In later developments of the model [22], the pressure drop equations were added to the system so that a hydraulic balance is also used. The combination of equations is occasionally referred to as the MERSHQ (Mass, Energy, Rate, Summation, Hydraulic, and energy(= Q)) equations.

The two film model of Whitman [23] assumes there are two stagnant film layers adjacent to the interface in both the vapor and liquid phases of thickness δ^V and δ^L . There is no convection in the film and the bulk concentrations outside the film boundary are perfectly mixed. There is an unrealistic discontinuity in concentration gradient at δ in both the liquid and vapor. In addition to the two film model, other models of interfacial behavior are available. Two of the most popular alternatives are the Higbie [24] model and the Danckwerts [25] model. These are both known as surface renewal models. While they are more complicated, they typically yield results that are within a few percent of the film model [25].

Discretizing Packed Columns

Application of the mass transfer model to random or structured packing requires the column height to be discretized into vertical segments or stages and the above equations solved for each segment n . (The term stages is used in many publications for these segments. These should not be confused with trays or equilibrium stages.) While there is no specific guidance on this process, some recommend the approximate value of HETP [26]. However, shorter segments may be appropriate when properties or composition change rapidly [27]. The model for packed towers is countercurrent flow in both the vapor and liquid and the number of segments can be viewed as an estimate of the amount of back-mixing, with large numbers of segments indicating no back-mixing and smaller numbers increased back-mixing [28]. The selection of this value can have significant impact on the results and consequently is one of the values that must be chosen cautiously in the mass transfer model. Collocation methods can be used to integrate the tower height and thus eliminate the requirement of discretization [29]. By assuming no back mixing, collocation can have the same effect as using a large

number of segments (i.e., plug flow in each phase). Alternatively, back mixing can be included through the use of dispersion terms [30].

The impact of the number of calculation segments in packed towers is shown in Figure 1. Figure 1 represents the performance as predicted by ProMax [1] of a Stahl column used in triethylene glycol regeneration packed with 1 in Pall rings. Water content of the regenerated glycol is presented at various packing depths in the Stahl column. The stripping gas rate is held constant at 3 SCF gas/gal TEG. At a segment height of 1 in, the residual water in the TEG is less than half the amount (on a molar basis) of using 12 in segments for most of the packing depth. For comparison, two ideal stages give a residual water content of slightly more than 1 mole %.

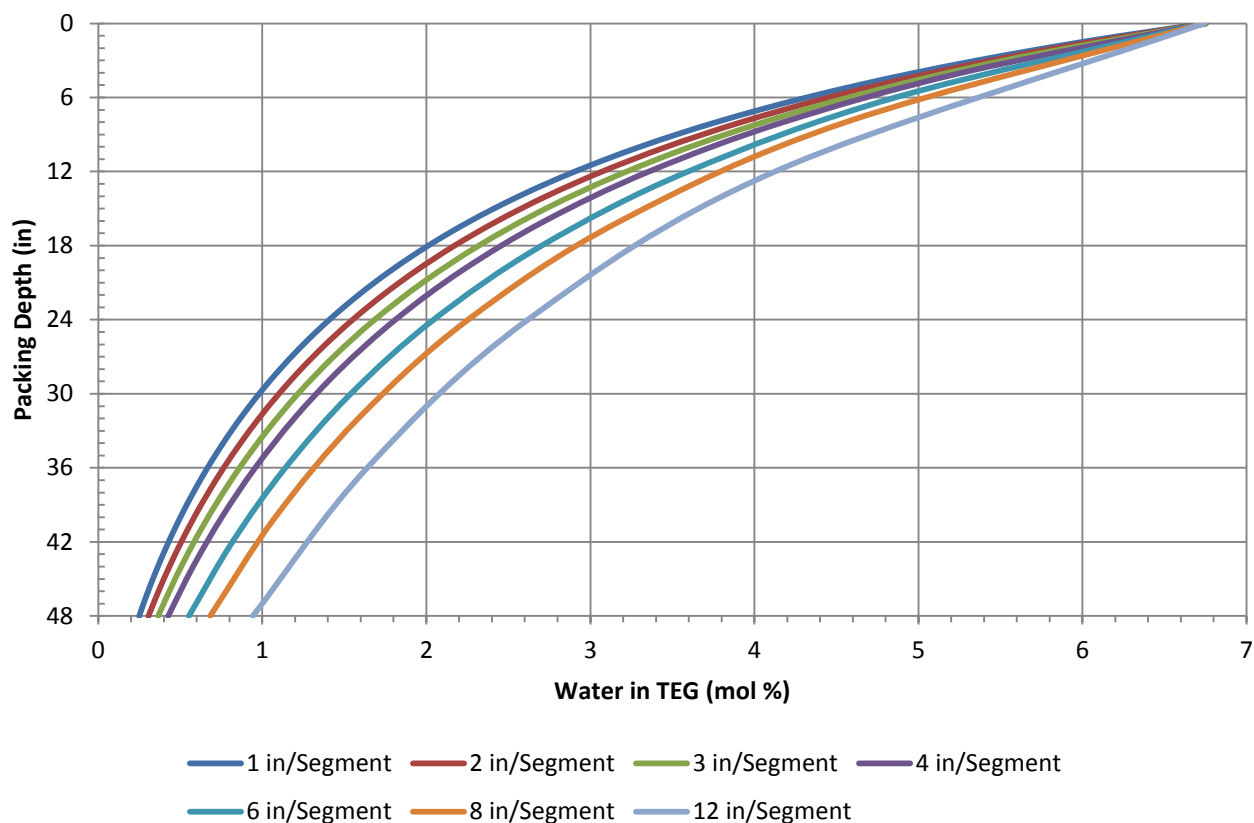


Figure 1 - The Effect of Packing Calculation Segment Height on Triethylene Glycol Regeneration Using 3 SCF/gal Stripping Gas

Tray Mixing Models

For trayed columns, various mixing models can be used for the liquid and vapor phases just as they can be used to calculate Murphree efficiencies in the ideal stage model [31]. The most basic assumption is that of complete mixing in both the liquid and vapor phases. This was the model used by Krishnamurthy and Taylor in the original development. However, the concentration gradients that develop on a tray can significantly impact the predictions made by this model due to the fact that this gradient is the driving force for mass transfer. As the column diameter becomes larger, the perfectly mixed flow model is less applicable. Kooijman and Taylor [32] show that for a specific depropanizer, the mixed flow model under predicts the Murphree tray efficiencies at approximately 60% for most components when the actual values should be near 100%. They provide an alternate plug flow model for the vapor. In addition, they provide a plug flow model for the liquid and an alternative axial

dispersion model for the liquid. Using these models, the efficiencies are brought closer to the expected values.

This mixing behavior is illustrated in Table II where the efficiency impact on product compositions from the nonequilibrium stage model and ideal stage model for an industrial scale butane splitter with 74 V-1 valve trays reported by Klemola and Ilme [33] and Ilme [34] are compared. For

Table II - Product Comparison of a 74 Tray Butane Splitter between Ideal Stage and Mass Transfer Models using Mixed Phases [33, 34].

| | Trays in Simulation | i-Butane in Distillate (wt %) | n-Butane in Bottoms (wt %) |
|-------------------------------|---------------------|-------------------------------|----------------------------|
| Operating Data (Actual Trays) | | 93.5 | 98.1 |
| Ideal Stage (PR EOS) | 74 | 93.5 | 97.9 |
| Mass Transfer (AIChE) | 74 | 91.9 | 97.1 |
| Ideal Stage (PR EOS) | 82 | 93.9 | 98.1 |
| Mass Transfer (AIChE) | 106 | 93.9 | 98.1 |

this case, the mass transfer model of ProMax [1] with a perfectly mixed flow model and AIChE mass transfer coefficients yields component vapor phase Murphree efficiencies of approximately 77% for both isobutane and normal butane for most trays in the column (see Figure 2). As mentioned in the discussion following equation (10), near equal efficiencies would be expected for these isomers. Since $\lambda \approx 1$ for this pseudo binary system of isomers, equation (11) indicates the overall column efficiency

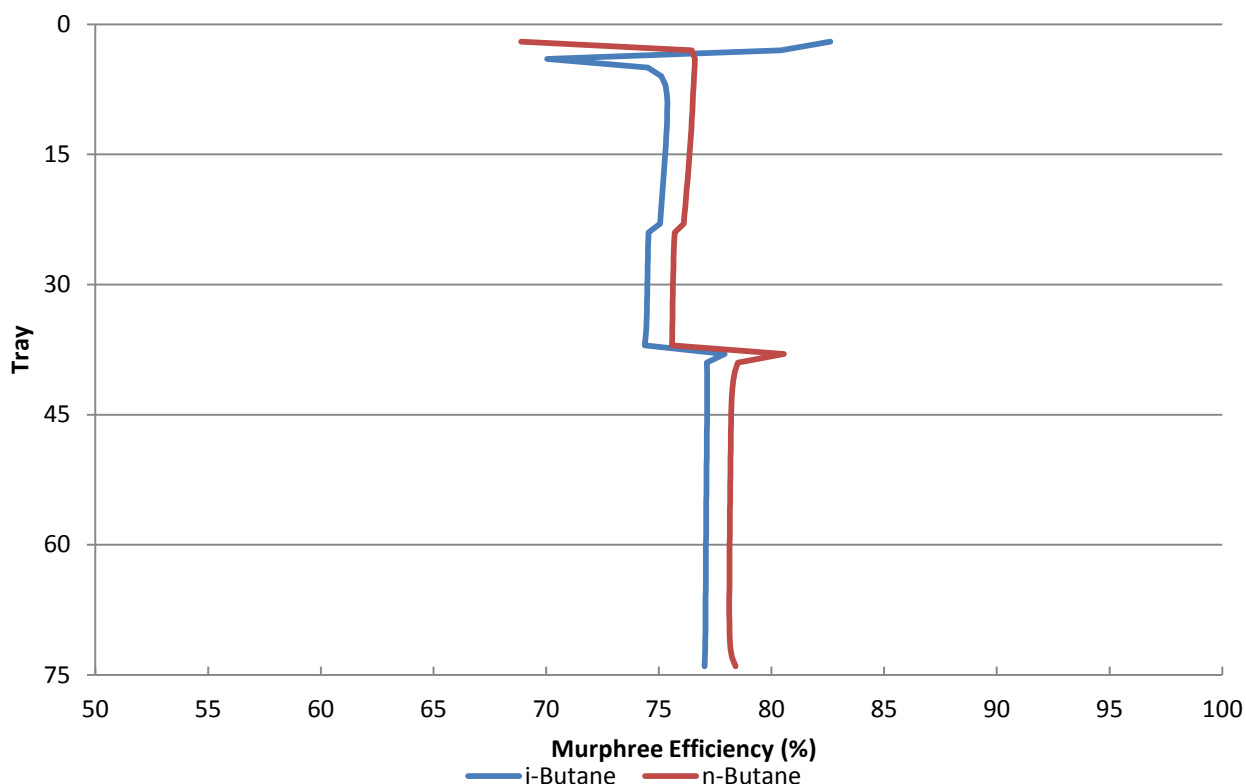


Figure 2 – Calculated Vapor Phase Murphree Efficiencies for i-Butane and n-Butane in 74 Tray Butane Splitter of Klemola and Ilme [33]

should be approximately 77% as well. However, Table II illustrates that even the ideal stage approach under predicts the performance of the unit. Based on the Peng-Robinson equation of state, a total of 82 trays for an overall column efficiency of approximately 110.8% are required to match the stated operating performance. Ilme uses a UNIFAC-SRK approach and arrives at an overall efficiency of 118.9% using 88 trays. For ProMax [1], the UNIFAC-Peng-Robinson approach gives a value of 102.3% based on 76 trays. For the mass transfer model, 106 trays would be required to match column performance for both key components.

Mass Transfer with Chemical Reaction

For modeling both liquid phase chemical reaction and mass transfer, Danckwerts [25] describes the use of the enhancement factor technique. The enhancement factor describes the increased rate of absorption due to the effect of a chemical reaction. It is defined as the ratio of the rate of absorption with the reaction occurring to the rate of absorption in the absence of the reaction. For the liquid phase the following equation is provided

$$N_{n,i}^L = E_{n,i} a_n k_{n,i}^L (x_{n,i}^I - x_{n,i}^L) \quad (16)$$

where $E_{n,i}$ is the appropriate enhancement factor. To determine $E_{n,i}$, the material balances for a reacting system are written which results in a differential equation due to the presence of the Fickian diffusion flux. The material balance requires kinetic rate expressions for all chemical reactions occurring in the system. As with equations for a non-reacting system, an appropriate model for interface behavior must be used. Normally the film model is employed. For only the simplest kinetic systems can these differential equations be solved in closed form. Usually numerical integration or other approximations must be used to solve the equations. Weiland [35] presents in GPA Research Report RR-153 enhancement factor expressions for most of the reactions of interest in amine treating. These were derived using the approximation approach.

Physical property and kinetic information are required by both the ideal stage and mass transfer modeling techniques. Much of this information is available in the published literature. GPA research projects have been conducted to measure data required for amine treating. Table III describes some of

Table III - Summary of GPA Sponsored Research for Amine Treating

| Report | Title | Year |
|---------------|--|-------------|
| RR-151 | Reaction Kinetics of CO ₂ with MEA, DEA and MDEA and in MDEA-Based Blends | 1996 |
| RR-152 | Physical Properties of MEA, DEA, MDEA and MDEA-Based Blends Loaded with CO ₂ | 1996 |
| RR-153 | Enhancement Factors for Acid Gas Removal with Single and Mixed Amines | 1996 |
| RR-157 | Acid Gas Treating with Aqueous Alkanolamines Part I: A Mass Transfer Model for Predicting Rates of Absorption or Stripping of H ₂ S and CO ₂ in Aqueous MDEA, DEA and Blends of DEA and MDEA | 1997 |
| RR-158 | Acid Gas Treating with Aqueous Alkanolamines Part II: Physical Property Data Important in Modeling H ₂ S and CO ₂ Absorption into Aqueous DEA, MDEA and Blends of DEA and MDEA | 1997 |
| RR-159 | Experimental Absorption Rate Measurements and Reaction Kinetics for H ₂ S and CO ₂ in Aqueous DEA, MDEA and Blends of and Blends of DEA and MDEA | 1997 |

the more recent physical property and kinetic information that have been obtained through GPA sponsorship.

Binary Mass Transfer, Interfacial Area, and Heat Transfer Correlations

Many correlations have been developed for binary mass transfer coefficients and interfacial area. Table IV lists some of the most popular correlations for trays, random, and structured packing.

Table IV - Correlations for Binary Mass Transfer Coefficients in Various Types of Distillation Hardware

| Equipment | Correlation | Reference |
|---------------------------|--------------------|------------------|
| Trays | AIChE | 10 |
| | Chan-Fair | 36 |
| | Chen-Chuang | 37 |
| | Scheffe-Weiland | 38 |
| | Stichlmair | 13 |
| | Zuiderweg | 12 |
| Random Packing | Billet-Schultes | 39 |
| | Bravo-Fair | 40 |
| | Onda | 41 |
| Structured Packing | Billet-Schultes | 39 |
| | Rocha-Bravo-Fair | 42 |

Generalized correlations for binary mass transfer coefficients must be developed from experimental data measured for a variety of systems and a range of operating conditions using multiple devices. The Billet-Schultes [39] correlation for random and structured packing was developed using 46 test systems and liquid and vapor rates ranging over almost three orders of magnitude. A comparison of the measured versus calculated overall mass transfer unit from this model is given in Figure 3 [43]. The dashed lines show $\pm 30\%$ deviation. The majority of the data fall within this range although there are still some outliers. This represents the accuracy to which data used in the correlation can be reproduced. Other systems not used in the development of the correlation may or may not be reproduced to the same degree of accuracy.

Binary mass transfer coefficients calculated by different correlations may be similar in magnitude, or may differ a great deal. Figure 4, taken from Kvamsdal and Rochelle [44], shows the vapor and liquid mass transfer coefficients for CO₂ capture with MEA using #40 IMTP random packing calculated from two different correlations. In this case the vapor phase mass transfer coefficient calculated using the Billet-Schultes correlation is double that using the Onda correlation. Likewise different correlations calculate different interfacial areas. Figure 5, which is based on results given in a paper on using MEA for CO₂ capture by Faramarzi, et al. [45], shows the interfacial area can vary significantly depending on the correlation used.

Once all of the binary combinations of mass transfer coefficients are calculated from correlation, the multicomponent mass transfer coefficients must be calculated to solve the distillation system. This process considers the interaction of the various binary pairs similar to that used in the Stefan-Maxwell analysis for multicomponent diffusion coefficients. The result is a matrix of multicomponent mass transfer coefficients that is $(c-1) \times (c-1)$ in size (c is the number of components in the system). The text of Taylor and Krishna [16] provides the background for these calculations. Because of these calculations, the multicomponent mass transfer coefficients may be prone to more error than the binary coefficients on which they are based. In general, the following

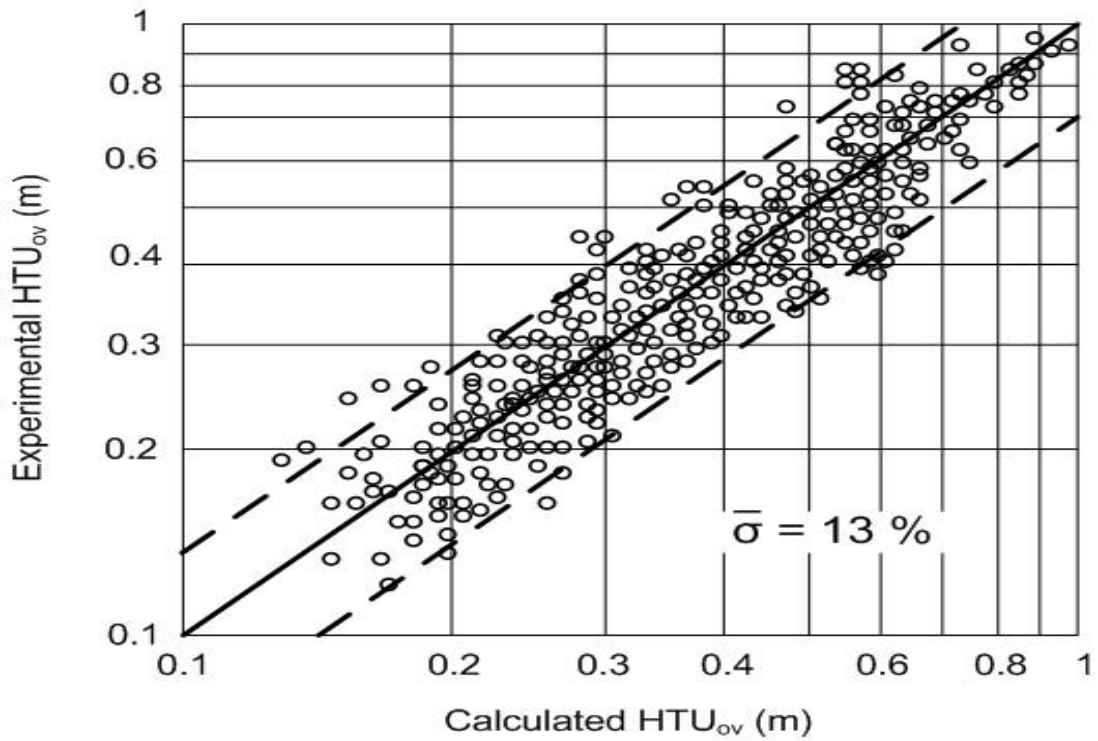


Figure 3 - Overall Gas Side Mass Transfer Unit Billet-Schultes Model [43]

quote by Wesselingh [46], reiterated by Taylor and Krishna in their 1993 text, should be kept in mind when using multicomponent mass transfer coefficient results:

“Our knowledge of multi-component transport coefficients is improving, but this is a slow process. I still occasionally have to pray that my estimate of some coefficient will not be off by more than one order of magnitude. Fortunately, this is usually not a major coefficient.”

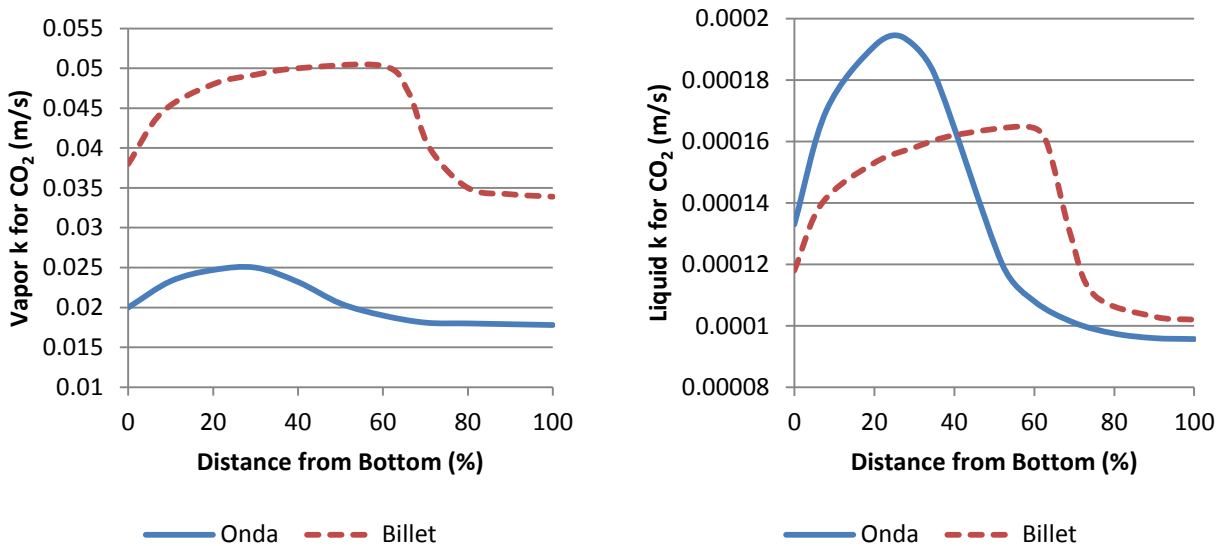


Figure 4 – Binary Vapor and Liquid Mass Transfer Coefficients for CO_2 Capture with MEA Correlation Comparison [44].

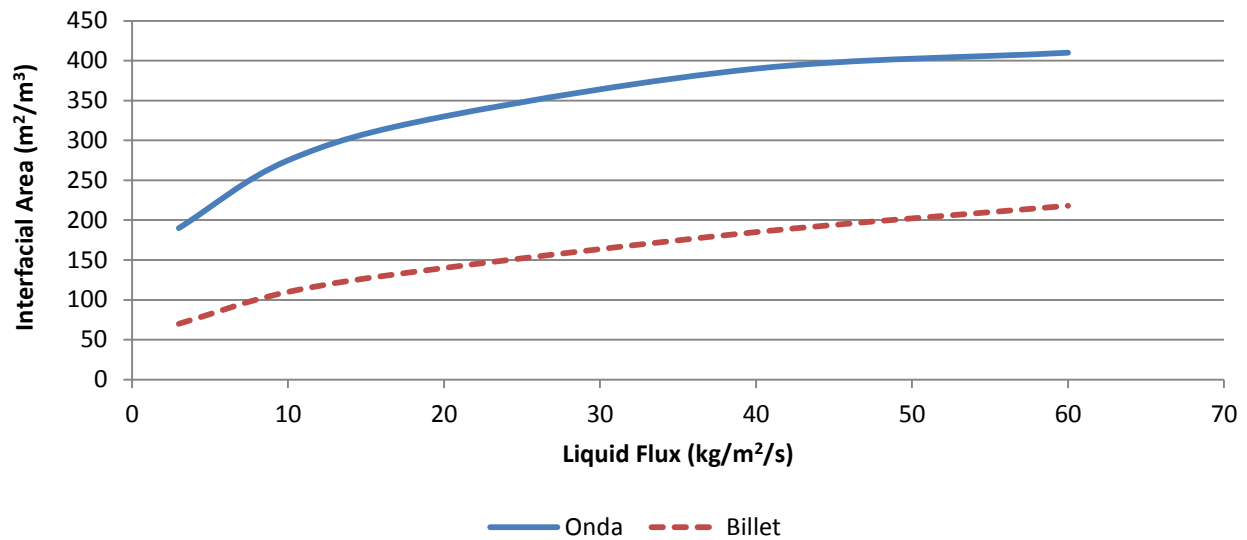


Figure 5 - Interfacial Area for CO₂ Capture on 13 mm Ceramic Berl Saddles Correlation Comparison [45].

The heat transfer coefficient for the vapor film is usually estimated from the Chilton-Colburn analogy, and for the liquid film either the Chilton-Colburn analogy or a penetration model can be used. These methods are normally not very accurate for heat transfer coefficient estimation, but it is rare to find heat transfer correlations that are applicable to this application. Fortunately, heat transfer coefficients do not appear to have much effect on predicted column performance [28], reducing the necessity for accurate predictions.

Mass transfer models require data necessary to calculate interphase mass and heat transfer coefficients and interfacial area based on correlations of the following transport and thermal properties: diffusivities, viscosities, densities, heat capacities, thermal conductivities, etc. Furthermore, mass transfer models require detailed information on the column internals. For trays this includes information such as weir heights and fraction active area and for packing this includes surface area per unit volume and void fraction. Although ideal stage models tend to have only a single equation per stage which needs to be solved in the inner loop, mass transfer models have more than 50 equations per stage. Because of these additional equations, a mass transfer model can take much longer to solve than an ideal stage model. Seader and Henley [47] state “computing time for a rate-based model is not generally more than an order of magnitude greater than that for an equilibrium-based model.”

APPLICATIONS OF MODELS TO INDUSTRIAL CASES

The two different modeling techniques are best compared by using a variety of examples of industrial interest. Both the ideal stage and mass transfer methods have been implemented in ProMax 4.0 beta version [1] for separation columns with and without chemical reactions. All results presented are made with this simulator. For most of the examples, columns using the two techniques were set up side by side with identical feeds, duties, and specifications. Unless otherwise stated, the results presented are from the best performing mass transfer correlation from the applicable alternatives.

Demethanizer

Demethanizers are often used to separate natural gas liquids (NGL's) from methane and lighter gases. Experimental data are available for a four foot diameter chemical plant demethanizer in FRI Plant Test Report No. 19 [48]. Thirty bubble cap trays were used with 18 inch tray spacing and a 2.5 inch outlet weir. This column produced an overhead product consisting of methane, hydrogen, and ethylene and a bottoms product containing ethylene, ethane, propylene, and propane. The ethylene recovery to the bottoms product ranges from 62-74%, depending on mass balance assumptions. (There is a 19% difference in measured feed and product ethylene rates).

The column configuration consisted of two feeds, a reflux stream, and a reboiler. Table V summarizes operating conditions and settings of the two models. The mass transfer calculation was

Table V - Demethanizer Calculated by Ideal Stage and Mass Transfer Model

| | Ideal Stage | Mass Transfer |
|------------------------------|--------------|---------------|
| Number of Stages | 15 | 30 |
| Overall Efficiency | 50% GPSA [6] | - |
| Overhead P, psig | 461 | 461 |
| Bottoms rate, Mlb/h | 24 | 24 |
| Bottoms Ethylene Recovery, % | 63 | 63 |

made using the AIChE [10] mass transfer coefficient correlation (all applicable correlations produced similar results).

Figure 6 provides a comparison of the composition profile calculated by the ideal stage model

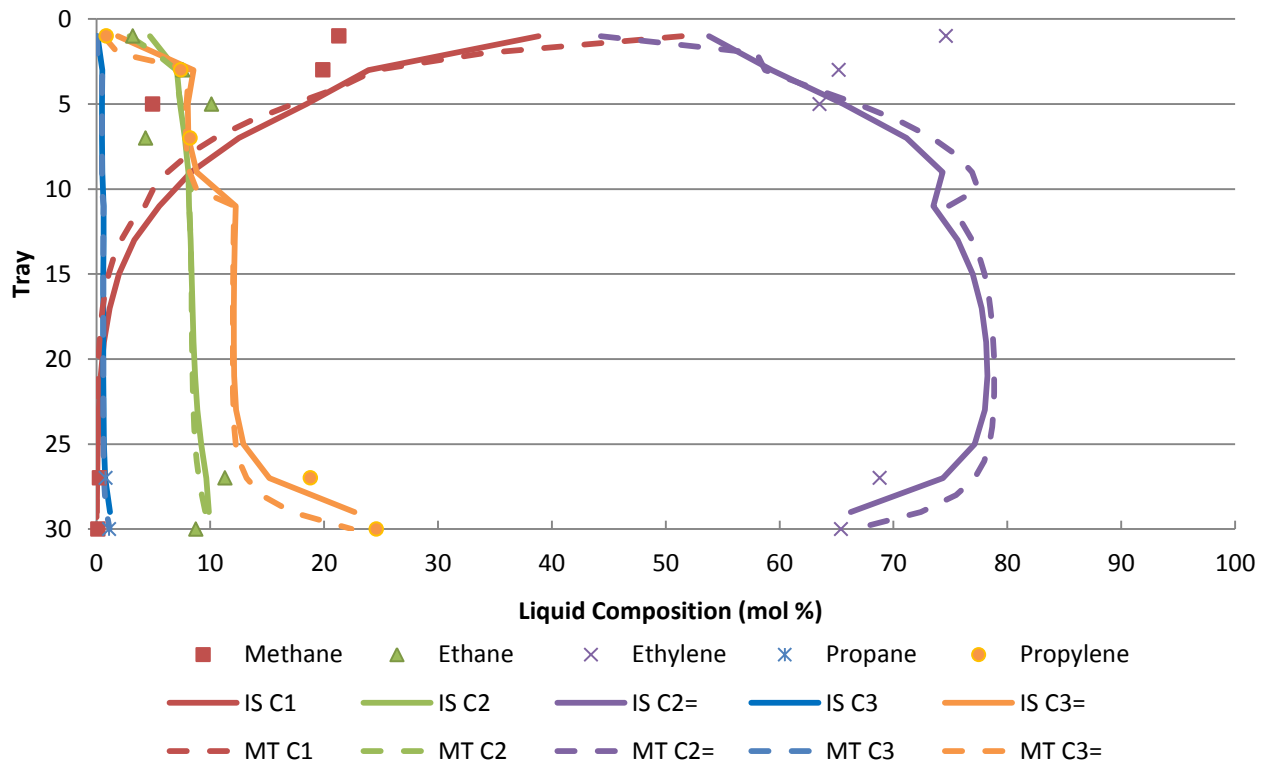


Figure 6 - Comparison of Demethanizer Tray Composition Profiles for Ideal Stage (IS) and Mass Transfer (MT) Models vs. Measured Values [48].

and the mass transfer model to the measured composition. The measured and calculated compositions are for the liquid phase. The composition profiles calculated by each model are similar and are in reasonable agreement with the somewhat scattered measurements. The feed composition which was chosen for the simulation is consistent with a 62% ethylene recovery in the bottoms product. Both models calculate a bottoms product ethylene recovery of 63%. Figure 6 indicates that both the ideal stage model with the expected efficiency and mass transfer model predict very similar results for this unit.

Glycol Dehydration

TEG absorbers are used for dew point control to remove the water from wet natural gas. Historically columns with bubble cap trays have been employed but structured packing has been increasingly used in this service. Valuable pilot plant data have been published by Kean et al. [49] which describes the test results of different structured packings at several bed depths and glycol concentrations. Figure 7 compares data from a 17 foot unit using the structured packing Flexipac II in a 14 in diameter column operated at 650 psig with 99.95 wt. % TEG at 90°F to predictions from the ideal stage and mass transfer models. The GPSA Engineering Data Book [7] gives the following guidelines for estimating HETP: “For random and structured packing, Height of Packing Equivalent to a Theoretical Plate (HETP) varies with TEG circulation rate, gas rate, gas density, and packing

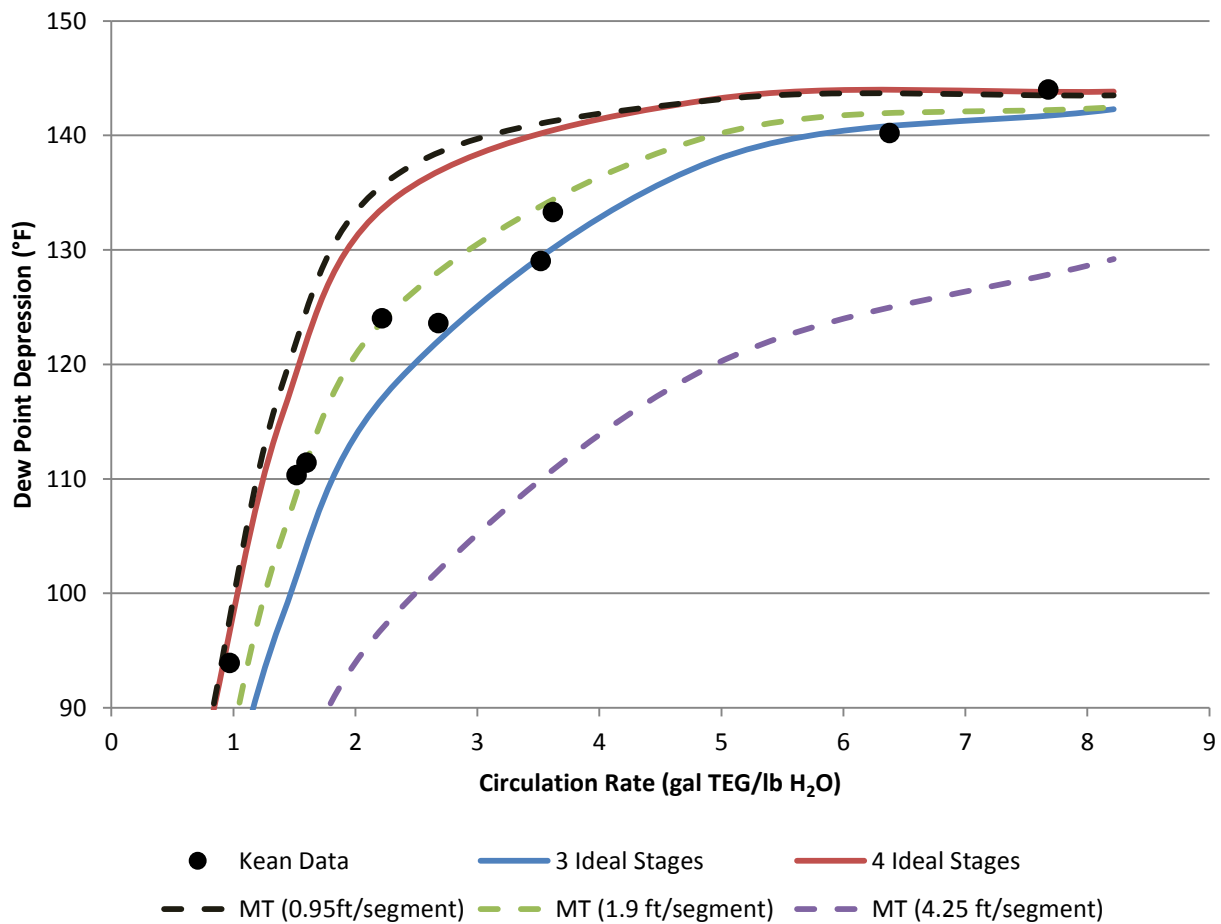


Figure 7 - Comparison of Mass Transfer (MT) and Ideal Stage Calculated TEG Dew Point Depressions with Experimental Results of Kean et al. [49].

characteristics but a value of about 60 in is usually adequate for planning purposes.” This would suggest between 3 and 4 ideal stages should be used. The measured dew point data fall within this range. The mass transfer results were calculated using the Billet-Schultes mass transfer coefficient model specifying the bed length, packing type, column diameter and 0.95, 1.9 and 4.25 ft segment heights. A segment height of 5 ft would correspond to one HETP which follows the recommendations of Subawalla and Fair [26]. The mass transfer model using 1.9 ft/segment predicted dew point depressions that match the measured performance well. As can be seen from the figure, using shorter segments does not ensure greater accuracy as the dew point depression is over predicted by using 0.95 ft/segment. The results indicate that segment length selection will be important in modeling this unit. Figure 7 also indicates that the ideal stage model accurately predicts the performance of the unit to be between three and four ideal stages as would be expected from the recommended HETP of 5 ft.

Quench Tower

Direct contact heat transfer can be advantageously used to cool a gas stream while minimizing pressure drop. For example, packed towers are sometimes used as interstage coolers in multistage compression. Strigle [50] describes a random packed tower which uses water to cool a hot gas from 196°F to 97°F. The necessary water flow rate is determined by heat balance. #70 IMTP packing is selected and the column diameter is chosen to yield an acceptable pressure drop. What remains to be determined is the required bed length. The bed length is calculated by dividing the cooling load by the product of the average volumetric heat transfer coefficient, the area, and the log mean temperature driving force. Strigle determined that a 17 foot bed of #70 IMTP random packing is required. The required bed length can also be calculated using the mass transfer model, which calculates both heat and mass transfer. Figure 8 shows the outlet gas temperature obtained using various bed lengths calculated with three different mass transfer correlations and 2 ft/segment. The resulting bed length agrees well with Strigle’s result using Billet-Schultes method. While all correlations tend to converge to the same point as expected (due to the energy balance), the outlet temperatures obtained for various columns lengths are somewhat different. The calculated temperature profile given in Figure 9 for the

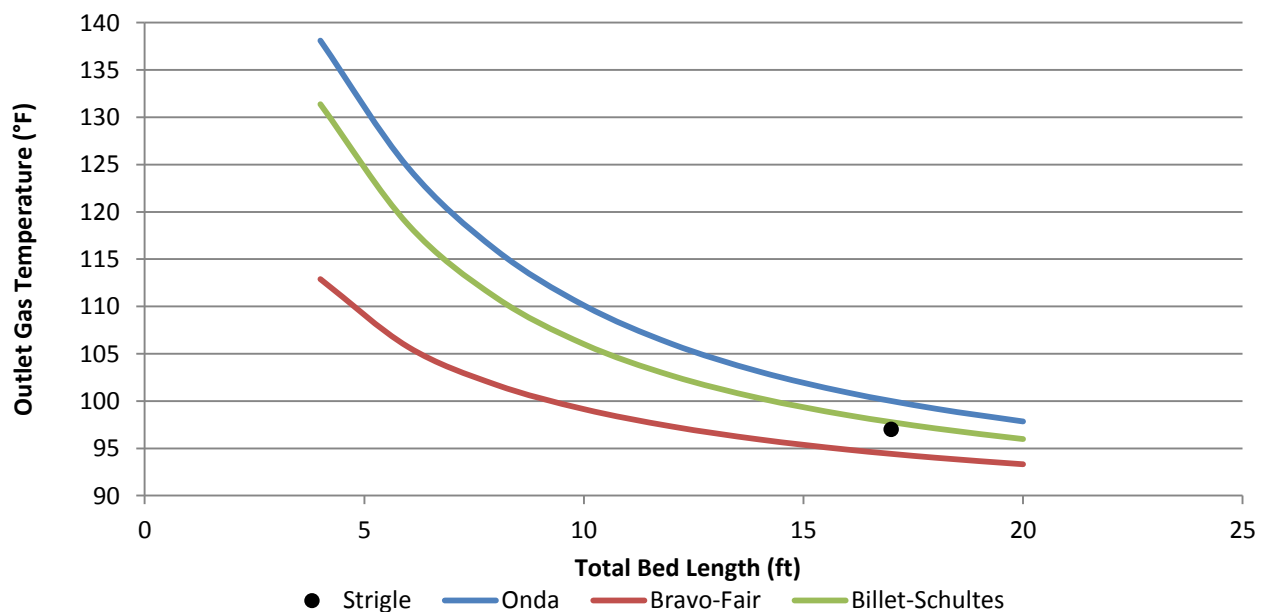


Figure 8 - Calculated Quench Tower Outlet Temperature vs. Total Bed Length and Results of Strigle [50].

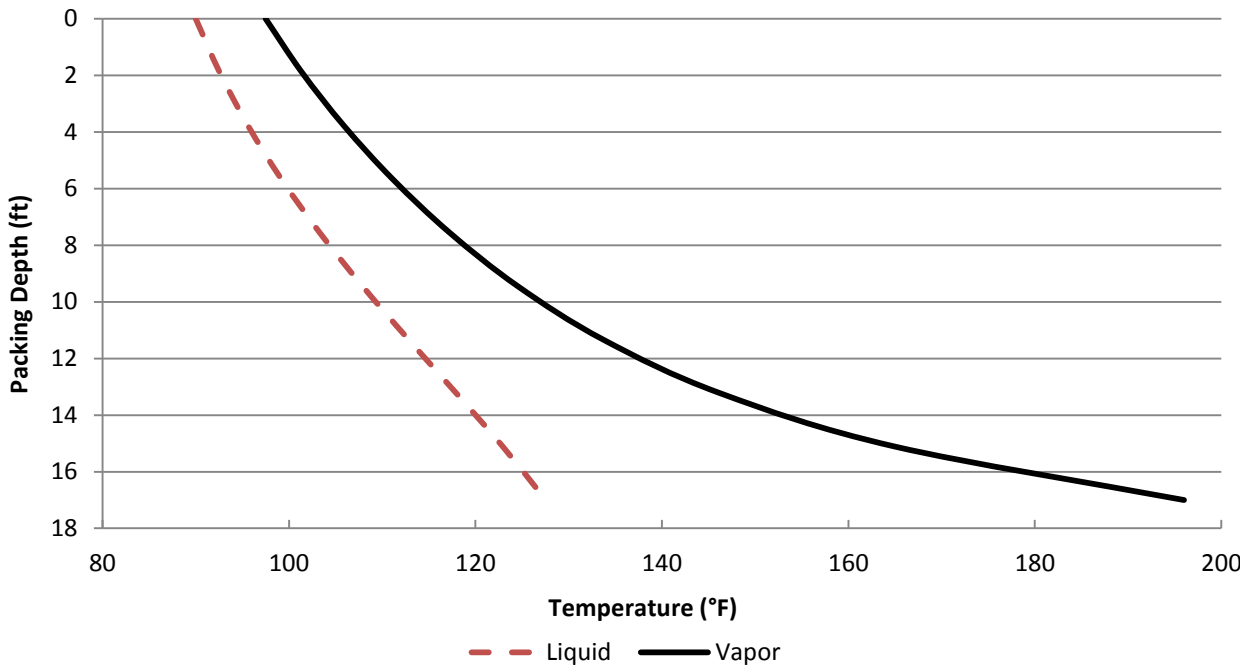


Figure 9 - Calculated Quench Tower Liquid and Vapor Temperature Profiles for 17 ft Column.

17 foot bed using Billet-Schultes and 9 segments shows the temperature difference between the vapor and liquid decreases as the vapor moves up the bed.

Butyl Acetate Synthesis via Reactive Distillation

Reactive or catalytic distillation has gained greatly in popularity over the past 20 years [51]. A major benefit of this process is that it can combine the actions of several different unit operations (a reactor and distillation columns to separate the reactants and products) into a single distillation column which can significantly reduce capital costs [52]. Both tray and packed columns can be used for reactive distillation. For catalytic reactions the catalyst can either be the packing itself or, for structured packings, can be embedded within the packing. One example of a reactive distillation column is that of the production of butyl acetate from the catalytic reaction of butanol and acetic acid [53]:



The unit consisted of a 50 mm diameter column with a reboiler and a total condenser with decanter, 6 m tall packed with Sulzer BX structured packing in the rectifying and stripping sections and Katapak-S structured packing (with an embedded catalyst) in the central reactive zone. Mass transfer was calculated using the Rocha-Bravo-Fair [42] correlation. Billet-Schultes provided similar results. UNIQUAC was used to calculate liquid phase thermodynamic properties. The gas phase was treated as an ideal gas. Figure 10 shows a comparison of the calculated and measured butanol conversions using four types of calculation methods: mass transfer with kinetic reactions, phase equilibrium with kinetic reactions, mass transfer with equilibrium reactions and phase equilibrium with equilibrium reactions. The number of calculation segments was determined using the recommended [53] segment heights of 0.2 m for the Sulzer BX packing and 0.25 m for the Katapak-S packing.

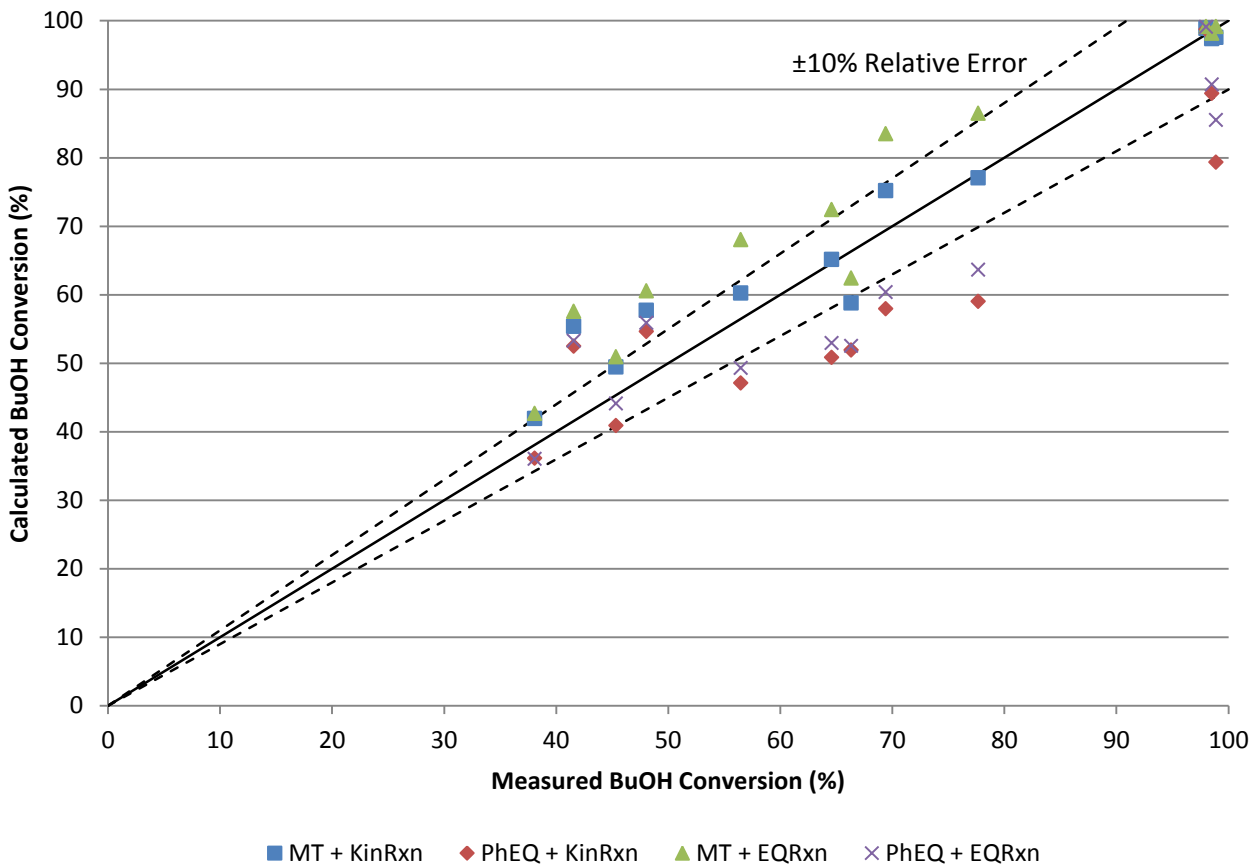


Figure 10 - Comparison of Calculated and Measured Butanol Conversions. (MT = Mass Transfer, PhEQ = Phase Equilibrium, KinRxn = Kinetic Reaction, EQRxn = Equilibrium Reaction).

Although for this particular case the calculated results using ProMax [1] indicate that a best fit was obtained using mass transfer and kinetic reactions, other simulations of reactive distillation columns have resulted in better fits assuming phase equilibrium or reaction equilibrium. In order to obtain a best fit of experimental data it is useful to be able to compare results using all of these options. ProMax allows for all of these combinations to be investigated.

As might be expected in columns in which reactions occur, the composition and temperature profiles can vary considerably within the column. Figure 11 shows a comparison of the calculated and measured composition and temperature profiles within the column for one of the experiments. Butanol was fed into the column on stage 6 and acetic acid was fed into the column on stage 10. The reaction zone consisted of stages 6 through 21. Stage 1 is the condenser and stage 28 is the reboiler. The results indicate that both the composition and temperature profiles for this reactive system are predicted well by ProMax.

Amine Treating Using MDEA

Sour gas containing H₂S and CO₂ is often sweetened by using amines such as MDEA. Daviet et al. [54] describe Dome's North Carolina Plant operations where 33 wt% MDEA is used in a 20 valve tray column to sweeten an inlet gas containing 50 ppm H₂S and 3.5% CO₂ to pipeline specifications. Tests were performed at varying amine flow rates resulting in various sweet gas compositions. The comparison below is for test number 5. The ideal stage-kinetics (historically called TSWEET kinetics and abbreviated herein as IS-K) calculation uses 7 ideal stages with reaction kinetics

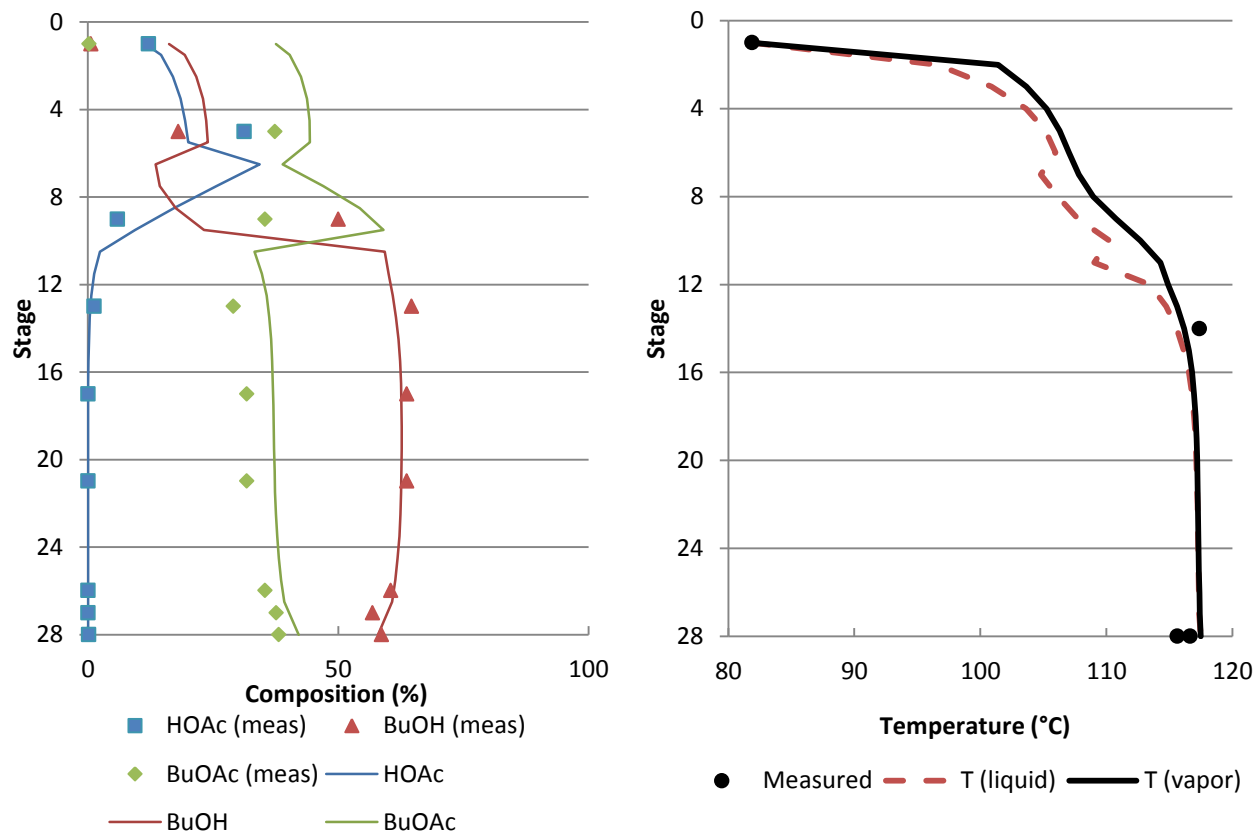


Figure 11 - Comparison of Calculated and Measured Composition and Temperature Profiles for Butyl Acetate Synthesis Using Mass Transfer and Kinetic Reaction (Run S1-6).

to account for kinetic effects on CO₂ absorption. The mass transfer-kinetics (MT-K) calculation uses 20 actual trays.

The results are summarized in Table VI for three different mass transfer correlations (the only three from Table IV which allow independent calculation of the interfacial area). A similar sweet gas composition is predicted by each model and is in good agreement with the measured composition. Figure 12 shows the calculated CO₂ profile from the two approaches is similar.

Reaction of the acid gases with the amine solutions generates heat and the temperature effects can be important. Figure 12 also compares the measured temperature profile to the model predictions. The mass transfer model shows the falling liquid is cooler than the rising vapor at the top of the column and the liquid is hotter than the vapor at the bottom of the column for all mass transfer

Table VI - Sweet Gas Composition

| | | Mass Transfer-Kinetics | | | |
|-----------------------|----------|------------------------|-----------|------------|-----------------|
| | | Ideal Stage-Kinetics | Zuiderweg | Stichlmair | Scheffe-Weiland |
| Test No. 5 | Measured | | | | |
| H ₂ S, ppm | <0.1 | 3.3 | 1.55 | 2.21 | 1.92 |
| CO ₂ , % | 1.13 | 1.23 | 1.19 | 1.16 | 0.94 |

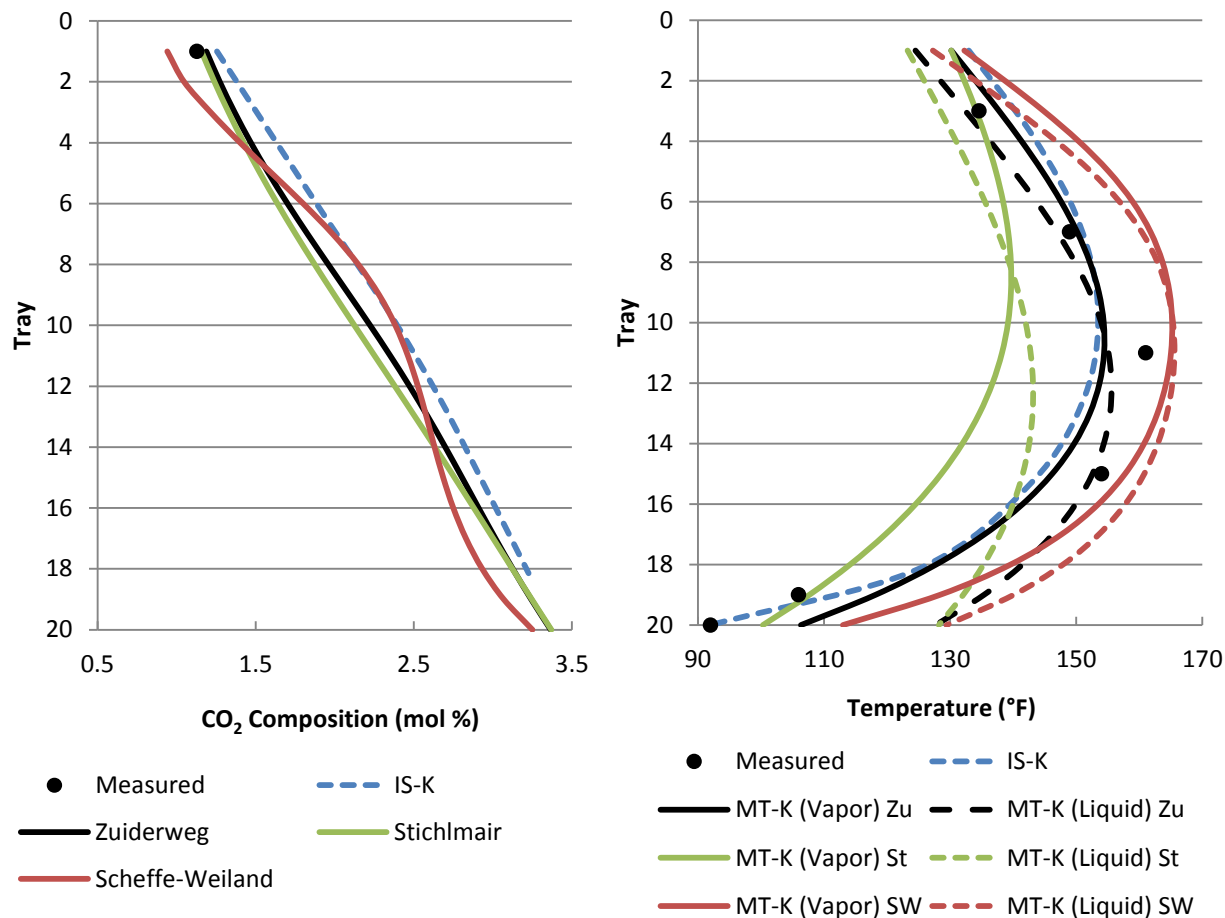


Figure 12 - Comparison of CO₂ Composition and Temperature Profiles in MDEA Column Using Ideal Stage-Kinetics (IS-K) and Mass Transfer-Kinetics (MT-K) models with the Zuiderweg (Zu), Stichlmair (St), and Scheffe-Weiland (SW) mass transfer correlations.

correlations. The ideal stage-kinetics results are similar to the vapor phase temperature from the mass transfer-kinetics model using the Zuiderweg mass transfer correlation. The Stichlmair correlation predicts lower temperatures, while the Scheffe-Weiland correlation predicts higher temperatures. The ideal stage-kinetics model provides the best prediction of the temperature profile. In this tower, the top four temperature sensors are in the vapor phase while the bottom two are in the liquid phase. Consequently, Zuiderweg produces similar results to the ideal stage-kinetics model for the vapor sensors, but over predicts the temperatures for the bottom sensors in the liquid phase.

CO₂ Removal Using MEA

MEA has been successfully used to remove both H₂S and CO₂ from sour natural gas and to recover CO₂ for use in the food industry. MEA is also being studied for use in capturing CO₂ from flue gas for carbon sequestration. Excellent operating data on a large pilot facility are given in the paper by Dugas et al. [55] which gives measured composition and temperature profiles for a packed bed absorber which uses a 17 m long bed of #50 IMTP random packing divided into four sections. An ideal stage-kinetics model calculation was performed using 12 stages and a residence time of 3 sec per stage. The mass transfer-kinetics model calculation was performed using 28 segments with 2 foot

packing per segment height and the Billet-Schultes, Onda, and Bravo-Fair mass transfer coefficient correlations. The results of the Onda and Bravo-Fair correlations were very similar to each other. Thus the Onda results are not presented.

As shown in Figure 13, both the ideal stage-kinetics and mass transfer-kinetics models predict the correct CO₂ removal, with the mass transfer model using the Billet-Schultes correlation predicting a slightly more accurate sweet gas composition (top point of the figure). The mass transfer-kinetics

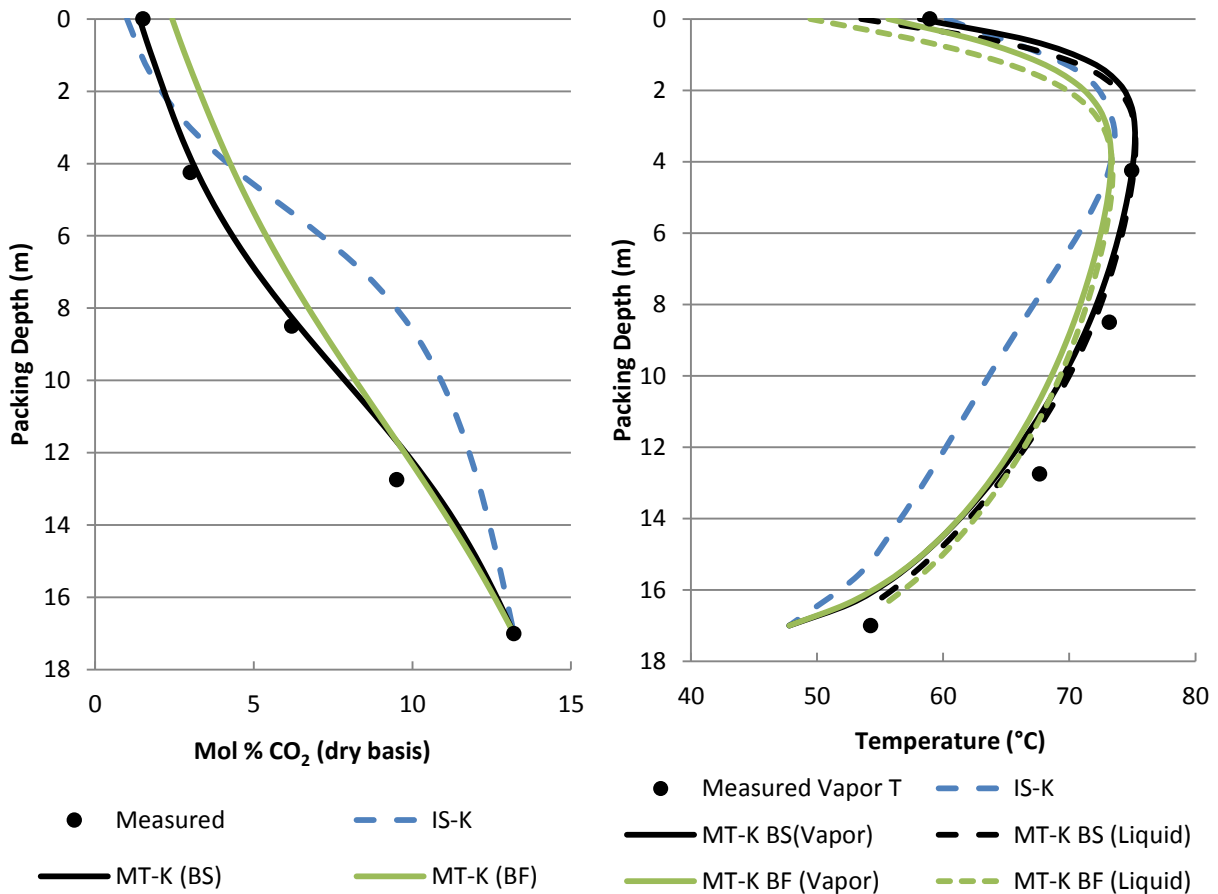


Figure 13 - Comparison of CO₂ Composition and Temperature Profiles in MEA Column Using Ideal Stage-Kinetics (IS-K) and Mass Transfer-Kinetics (MT-K) models with Billet-Schultes (BS) and Bravo-Fair (BF) mass transfer coefficient correlations.

model also better matched the overall composition profile. Also shown in Figure 13, both models predict accurate overhead sweet gas temperatures, and the temperature profile is better matched by the mass transfer-kinetics model for this case.

Although not shown in the interest of space, the effect of packing segment height was also investigated for this MEA unit as in the glycol absorber presented earlier. Unlike the glycol unit, the impact on composition was minor for reasonable values of segment height. The effect on temperature profile was greater than composition, but still only a maximum change of approximately 5°C was noted.

CONCLUSIONS

When performed properly, both the ideal stage and mass transfer approach as implemented in ProMax 4.0 can calculate accurate results for a variety of separation processes with and without reactions. The ideal stage approach can be used initially to determine appropriate equipment sizes and operating conditions. More detailed studies can be performed using the ideal stage approach, the mass transfer approach, or both. Advantages of the ideal stage approach include ease of use (equipment design details not required), speed of calculation, and minimum amount of data needed. Although significant operating experience provides reasonable efficiency estimates for most processes, the empiricism in scaling up from ideal to real stages or ideal stages to real bed lengths can be a disadvantage when accurate overall efficiencies or HETP's are unavailable. The mass transfer approach requires more equipment design details and does not make use of overall efficiencies or HETP's. More detailed composition and temperature profiles are produced by this method at the expense of longer calculation time. The mass transfer approach may appear more predictive in nature, but is not necessarily more accurate. It relies on more parameters that must be estimated, as both require thermodynamic data to model equilibrium—for the tray composition in the ideal stage approach and for the interface composition in the mass transfer approach. Many of these mass transfer parameters are of limited accuracy but also may be of limited sensitivity in some systems. Both techniques are useful tools in process simulation.

REFERENCES CITED

1. *ProMax 4.0 Development Beta*, Bryan Research and Engineering, Inc., 2012.
2. Taylor, R., Krishna, R., and Kooijman, H.A., "Modeling of Distillation", *Chem. Eng. Prog.*, **99**, 28, 2003.
3. Ponchon, M., "Etude Graphique de la Distillation Fractionnée Industrielle," *Tech. Mod.*, **13**, 20, 1921.
4. Savarit, R., "Elements de Distillation," *Arts et Métiers*, **75**, 65, 142, 178, 241, 266, 307, 1922.
5. McCabe, W.L., and Thiele, E.W., "Graphical Design of Fractionating Columns," *Ind. Eng. Chem.*, **17**, 605, 1925.
6. *Engineering Data Book*, 12th ed., Section 19—Fractionation and Absorption, Gas Processors Suppliers Association, Tulsa, OK., 2004.
7. *Engineering Data Book*, 12th ed., Section 20—Dehydration, Gas Processors Suppliers Association, Tulsa, OK., 2004.
8. O'Connell, H.E., "Plate Efficiency of Fractionating Columns and Absorbers," *Trans. Am. Inst. Chem. Engrs.*, **42**, 741, 1946.
9. Murphree, E.V., "Rectifying Column Calculations with Particular Reference to N Component Mixtures," *Ind. Eng. Chem.*, **17**, 747, 1925.
10. AIChE, *Bubble Tray Design Manual: Prediction of Fractionation Efficiency*, AIChE, New York, 1958.
11. Lockett, M.J., *Distillation Tray Fundamentals*, Cambridge University Press, Cambridge, 1986.
12. Zuiderweg, F. J. "Sieve Trays: A View on the State of the Art," *Chem. Eng.Sci.*, **37**, 1441, 1982.
13. Stichlmair, J.G., and Fair, J.R., *Distillation: Principles and Practices*, Wiley-VCH, New York, 1998.
14. Lewis, W.K., Jr., "Rectification of Binary Mixtures," *Ind. Eng. Chem.*, **28**, 402, 1936.

15. Toor, H.L., "Prediction of Efficiencies and Mass Transfer on a Stage with Multicomponent Systems," *AICHE Journal*, **10**, 545, 1964.
16. Taylor, R., and Krishna, R., *Multicomponent Mass Transfer*, Wiley, New York, 1993.
17. Bird, R.B., Stewart, W.E., and Lightfoot, E.N., *Transport Phenomena*, John Wiley & Sons, New York, 1960.
18. Krishnamurthy, R., and Taylor, R., "A Nonequilibrium Stage Model of Multicomponent Separation Processes, Part I: Model Description and Method of Solution," *AICHE Journal*, **31**, 449, 1985.
19. Krishnamurthy, R., and Taylor, R., "A Nonequilibrium Stage Model of Multicomponent Separation Processes, Part II: Comparison with Experiment," *AICHE Journal*, **31**, 456, 1985.
20. Krishnamurthy, R., and Taylor, R., "A Nonequilibrium Stage Model of Multicomponent Separation Processes, Part III: The Influence of Unequal Component Efficiencies in Process Design Problems," *AICHE Journal*, **31**, 1973, 1985.
21. Krishna, R., and Standart, G.L., "Mass and Energy Transfer in Multicomponent Systems," *Chem. Eng. Commun.*, **3**, 201, 1979.
22. Taylor, R., Kooijman, H.A., Hung, J.-S., "A Second Generation Nonequilibrium Model for Computer Simulation of Multicomponent Separation Processes," *Computers Chem. Engng.*, **18**, 205, 1994.
23. Whitman, W.G., "The Two-Film Theory of Gas Absorption," *Chem. And Met. Eng.*, **29**, 146, 1923.
24. Higbie, R., "Penetration Theory Leads to Use of the Contact Time in the Calculation of the Mass Transfer Coefficients in the Two Film Theory," *Trans. Am. Inst. Chem. Engrs.*, **31**, 365, 1935.
25. Danckwerts, P.V., *Gas-Liquid Reactions*, McGraw-Hill, New York, 1970.
26. Subawalla, H., and Fair, J.R., "Design Guidelines for Solid-Catalyzed Reactive Distillation Systems," *Ind. Eng. Chem. Res.*, **38**, 3696, 1999.
27. Baur, R., and Krishna, R., "Hardware Selection and Design Aspects for Reactive Distillation Columns. A Case Study on Synthesis of TAME", *Chem. Eng. Proc.*, **41**, 445, 2002.
28. Peng, J., Lextrait, S., Edgar, T.F., and Fair, J.R., "A Comparison of Steady-State Equilibrium and Rate-Based Models for Packed Bed Reactive Distillation", *Ind. Eng. Chem. Res.*, **41**, 2735, 2002.
29. Noeres, C., Kenig, E.Y., and Gorak, A., "Modelling of Reactive Separation Processes: Reactive Absorption and Reactive Distillation," *Chem. Eng. Proc.*, **42**, 157, 2003.
30. Danckwerts, P.V., "Continuous Flow Systems – Distribution of Residence Times," *Chem. Eng. Sci.*, **2**, 1, 1953.
31. Higler, A., Krishna, R. and Taylor, R., "Nonequilibrium Cell Model for Multicomponent (Reactive) Separation Processes," *AICHE Journal*, **45**, 2357, 1999.
32. Kooijman, H.A., Taylor, R., "Modelling Mass Transfer in Multicomponent Distillation," *The Chemical Engineering Journal*, **57**, 177, 1995.
33. Klemola, K.T., Ilme, J.K., "Distillation Efficiencies of an Industrial-Scale i-Butane/n-Butane Fractionator," *Ind. Eng. Chem. Res.*, **35**, 4579, 1996.
34. Ilme, J., "Estimating Plate Efficiencies in Simulation of Industrial Scale Distillation Columns," Ph.D. Thesis, Lappeenranta University of Technology, 1997.
35. Weiland, R.H., "Enhancement Factors for Acid Gas Removal with Single and Mixed Amines," GPA Research Report RR-153, Gas Processors Association, Tulsa, OK., 1996.
36. Chan, H., and Fair, J.R., "Prediction of Point Efficiencies on Sieve Trays. 1. Binary Systems," *Ind. Eng. Chem. Process Des. Dev.*, **23**, 814, 1984.

37. Chen, G.X., and Chuang, K.T., "Prediction of Point Efficiency for Sieve Trays in Distillation" *Ind. Eng. Chem. Res.*, **32**, 701, 1993.
38. Scheffe, R.D. and Weiland, R.H., "Mass-Transfer Characteristics of Valve Trays" *Ind. Eng. Chem. Res.*, **26**, 228, 1987.
39. Billet, R., and Schultes, M., "Prediction of Mass Transfer Columns With Dumped and Arranged Packings—Updated Summary of the Calculation Method of Billet and Schultes" *Trans IChemE*, **77**, Part A, 498, 1999.
40. Bravo, J.L. and Fair, J.R., "Generalized Correlation for Mass Transfer in Packed Distillation Columns" *Ind. Eng. Chem. Process Des. Dev.*, **21**, 162, 1982.
41. Onda, K., Takeuchi, H., and Okumoto, Y., "Mass Transfer Coefficients Between Gas And Liquid Phases in Packed Columns," *J. Chem. Eng. Japan*, **1**, 56, 1968.
42. Rocha, J.A., Bravo, J.L., and Fair, J.R., "Distillation Columns Containing Structured Packings: A Comprehensive Model for Their Performance. 2. Mass-Transfer Model" *Ind. Eng. Chem. Res.*, **35**, 1660, 1996.
43. Billet, R., and Schultes, M., "Predicting Mass Transfer in Packed Columns," *Chem. Eng. Technol.*, **16**, 1, 1993.
44. Kvamsdal, H.M., and Rochelle, G.T., "Effects of the Temperature Bulge in CO₂ Absorption from Flue Gas by Aqueous Monoethanolamine," *Ind. Eng. Chem. Res.*, **47**, 867, 2008.
45. Faramarzi, L., Kontogeorgis, G.M., Michelsen, M.L., Thomsen, K., and Stenby, E.H., "Absorber Model for CO₂ Capture by Monoethanolamine," *Ind. Eng. Chem. Res.*, **49**, 3751, 2010.
46. Wesselingh, J.A., "How on Earth, Can I Get Chemical Engineers to do Their Multi-Component Mass Transfer Sums Properly?" *J. Membrane Sci.*, **73**, 323, 1992.
47. Seader, J.D., and Henley, E.J., *Separation Process Principles, 2nd Edition*, John Wiley & Sons, 2006.
48. Fractionation Research, Inc. Plant Test Report No. 19, "Efficiency Test of a 4 foot diameter demethanizer with bubble cap trays", 1963. Available from Oklahoma State University Library special collections.
49. Kean, J.A., Turner, H.M., and Price, B.C., "Structured Packing in Triethylene Glycol Dehydration Service", Proceedings – Laurance Reid Gas Conditioning Conference, 1991.
50. Strigle, Jr., R.F., *Random Packings and Packed Towers*, Gulf Publishing, Houston, TX, 1987.
51. Taylor, R., and Krishna, R., "Modelling Reactive Distillation", *Chem. Eng. Sci.*, **55**, 5183, 2000.
52. Siirola, J.J., "An Industrial Perspective on Process Synthesis", *A.I.Ch.E. Symposium Series No. 304*, **91**, 222, 1995.
53. Steinigeweg, S., and Gmehling, J., "*n*-Butyl Acetate Synthesis via Reactive Distillation: Thermodynamic Aspects, Reaction Kinetics, Pilot Plant Experiments, and Simulation Results", *Ind. Eng. Chem. Res.*, **41**, 5483, 2002.
54. Daviet, G.R., Sundermann, R., Donnelly, S.T., and Bullin, J.A., "Dome's NC Plant Successful Conversion to MDEA," 63rd Annual GPA Convention, New Orleans, LA, 1984.
55. Dugas, R., Alix, P., Lemaire, E., Broutin, P., and Rochelle, G., "Absorber Model for CO₂ Capture by Monoethanolamine — Application to CASTOR Pilot Results", *Energy Procedia*, **1**, 103, 2009.